Electronic Supplementary Material (ESI) for Journal of Materials Chemistry C.

Supplementary Information

Advantages and disadvantages of vacuum-deposited and spin-coated amorphous organic semiconductor films for organic light-emitting diodes

Maki Shibata,[a] Yoshiya Sakai[b] and Daisuke Yokoyama*[abc]

[a] Department of Organic Device Engineering, Yamagata University, 4-3-16 Jonan, Yonezawa, Yamagata 992-8510, Japan.

[b] Department of Polymer Science and Engineering, Yamagata University, 4-3-16 Jonan, Yonezawa, Yamagata 992-8510, Japan.

[c] Research Center for Organic Electronics (ROEL), Yamagata University, 4-3-16 Jonan, Yonezawa, Yamagata 992-8510, Japan

E-mail: d_yokoyama@yz.yamagata-u.ac.jp; Fax & Tel: +81-238-26-3890

List of table and figures

Table S1 Experimental conditions used for film fabrication and thicknesses of the film samples in each figure. All of the vacuum-deposited films were fabricated at a deposition rate of 2 Å s^{-1} except in Figs. 16, 17, S16, and S17.

Fig.	Material	Vac.[a]/Solvent	Solution concentration (mg ml^{-1})	Spin speed (rpm)	Thickness (nm)	Annealing temperature for transition (°C)[b]
3	TPD	vac.	–	–	51.8–204.5, 330.0	–
4	TPD	chloroform	2–15	1000–5000	6.7–107.1	–
6	TPD	vac.	–	–	52.3	–
		chloroform	15	4000	49.6	–
		toluene	15	2000	51.1	–
		chlorobenzene	15	1000	53.8	–
		o-dichlorobenzene	40	2000	56.3	–
7, 8	TPD	vac.	–	–	71.5	100
		chloroform	10	1000	66.0	100
9	TPD	vac.	–	–	47.0	100
		chloroform	10	2000	49.1	–
10, 15	2-TNATA	vac.	–	–	101.2	130
		chloroform	15	1000	103.8	130
11	2-TNATA	vac.	–	–	101.2	130
		chloroform	15	1000	103.8	–
12	2-TNATA	vac.	–	–	46.5	130
		chloroform	10	2000	47.8	–
13	2-TNATA	chloroform	10–20	1000–7000	30.7–150.0	–
14	2-TNATA	vac.	–	–	101.3	130
		chloroform	15	1000–7000	48.1–115.6	130
16, 17	2-TNATA	vac. (0.2 Å s^{-1})	–	–	106.3	150
		vac. (2 Å s^{-1})	–	–	100.8	150
		vac. (20 Å s^{-1})	–	–	112.8	150
18	TPD	chlorobenzene	30	1000	105.8	–
	TPT1	chlorobenzene	30	1000	102.4	–
	Poly-TPD	chlorobenzene	30	1000	108.4	–
19	TPD	chlorobenzene	30	1000	99.5	–
	TPT1	chlorobenzene	30	1000	106.7	–
	Poly-TPD	chlorobenzene	30	1000	104.7	–
S1	TPD	vac.	–	–	51.8–204.5	–
	α-NPD	vac.	–	–	51.7–201.2	–
	CBP	vac.	–	–	48.7–186.9	–
	Alq_3	vac.	–	–	51.7–201.2	–
	α-ONPD	vac.	–	–	51.9–146.1	–
	2-TNATA	vac.	–	–	47.8–192.8	–
	TPT1	vac.	–	–	52.4–159.4	–
	TSBF	vac.	–	–	49.2–149.8	–
	BDAVBi	vac.	–	–	50.6–140.6	–
S2	TPD	vac.	–	–	330.0	–
	α-NPD	vac.	–	–	305.5	–
	CBP	vac.	–	–	300.1	–
	Alq_3	vac.	–	–	273.9	–
S3	α-NPD	chloroform	2–15	1000–5000	6.1–100.0	–
	CBP	chloroform	2–15	1000–5000	6.4–100.0	–
	Alq_3	chloroform	2–15	1000–5000	8.0–99.8	–
	2-TNATA	chloroform	10–20	1000–7000	30.7–150.0	–
	TPT1	chloroform	10–20	1000–7000	27.7–148.0	–
S4	TPD	toluene	2–15	1000–5000	9.3–68.7	–
		chlorobenzene	2–15	1000–5000	7.4–51.0	–
		o-dichlorobenzene	20–40	1000–5000	18.1–80.0	–

(Continued on next page)

(Continued from the previous page)

Fig.	Material	Vac.[a]/Solvent	Solution concentration (mg ml^{-1})	Spin speed (rpm)	Thickness (nm)	Annealing temperature for transition (°C)[b]
S5	TPD	vac.	–	–	52.3, 102.2	–
S6	α-NPD	vac.	–	–	17.6	–
		chloroform	5	4000	17.2	–
		toluene	3	600	18.9	–
		chlorobenzene	4	500	19.8	–
S7, 9	α-NPD	vac.	–	–	64.2	120
		chloroform	10	1000	67.7	120
	TPT1	vac.	–	–	106.1	170
		chloroform	30	5000	115.4	170
	TSBF	vac.	–	–	103.4	250
		chloroform	30	3000	110.9	250
S8	α-NPD	chloroform	10	1000	62.5	130
	2-TNATA	chloroform	15	1000	103.0, 111.0	130
S10	α-NPD	vac.	–	–	44.2	120
		chloroform	10	2000	43.2	–
	TPT1	vac.	–	–	53.6	170
		chloroform	10	1000	56.0	–
	TSBF	vac.	–	–	102.9	250
		chloroform	20	2000	105.0	–
	BDAVBi	vac.	–	–	35.5	130
		chloroform	5	1000	36.3	–
S11	TPT1	vac.	–	–	106.1	170
		chloroform	30	5000	115.4	–
	TSBF	vac.	–	–	103.4	250
		chloroform	30	3000	114.7	–
	BDAVBi	vac.	–	–	96.9	130
		chloroform	15	1000	101.7	–
S12	TPT1	chloroform	10–20	1000–7000	27.7–148.0	–
		toluene	10–20	1000–7000	19.0–98.7	–
S13	TPT1	vac.	–	–	53.6	170
		chloroform	15	1000-7000	41.9–105.5	170
		toluene	15	1000-7000	27.8–62.5	170
S14	2-TNATA	chloroform	15	1000	103.8	–
		toluene	15	600	104.3	–
		chlorobenzene	30	1000	109.4	–
		o-dichlorobenzene	40	600	100.8	–
S15	2-TNATA	chloroform	10	5000	35.1	–
		toluene	10	1500	39.7	–
		chlorobenzene	10	1000	35.4	–
S16, 17	TPD	vac. (0.2 Å s^{-1})	–	–	94.5	100
		vac. (2 Å s^{-1})	–	–	100.3	100
		vac. (20 Å s^{-1})	–	–	100.5	100
S16	TPT1	vac. (0.2 Å s^{-1})	–	–	98.5	170
		vac. (2 Å s^{-1})	–	–	104.1	170
		vac. (20 Å s^{-1})	–	–	99.8	170
S18	TPD	vac.	–	–	49.0	100
S19	TPD	vac.	–	–	46.5	100
		chloroform	10	3000	45.9	100
	α-NPD	vac.	–	–	35.1	120
		chloroform	10	3000	39.1	120

[a] The vacuum-deposited films were fabricated at a deposition rate of 2 Å s^{-1} unless otherwise indicated.

[b] The temperatures at which the as-prepared films were annealed for 30 min to induce film transitions.

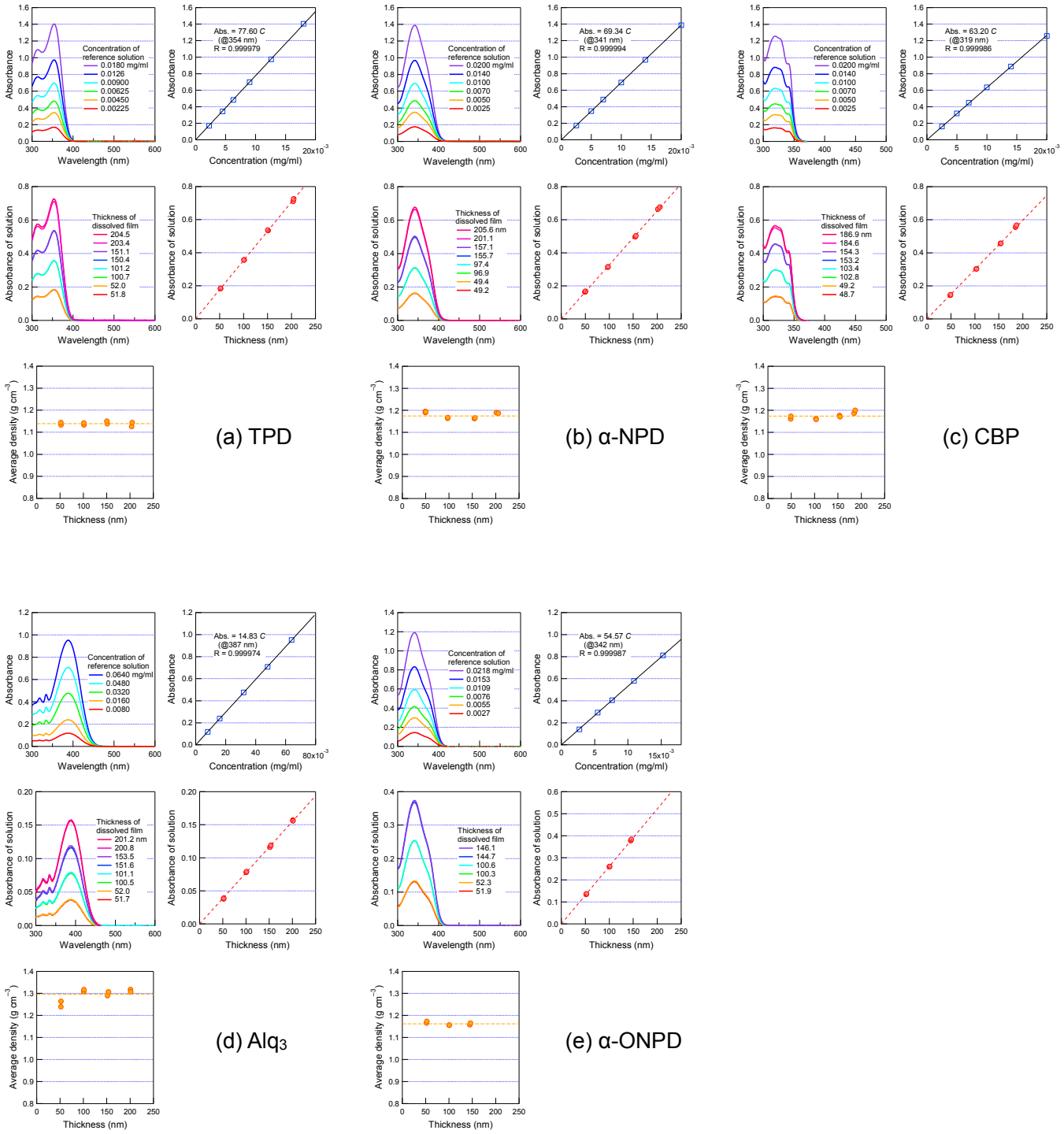

Fig. S1(a)–(e) UV-vis absorption spectra of reference solutions and solutions of dissolved vacuum-deposited films of (a) TPD, (b) α-NPD, (c) CBP, (d) Alq_3, and (e) α-ONPD. Each material has five figures. For each, the upper left shows the absorption spectra of the reference solutions, and the upper right shows the calibration line. The central left shows the absorption spectra of the solutions of the dissolved films, and the central right shows the dependence of the absorbance on film thickness. The lower left shows the density of films with different thicknesses.

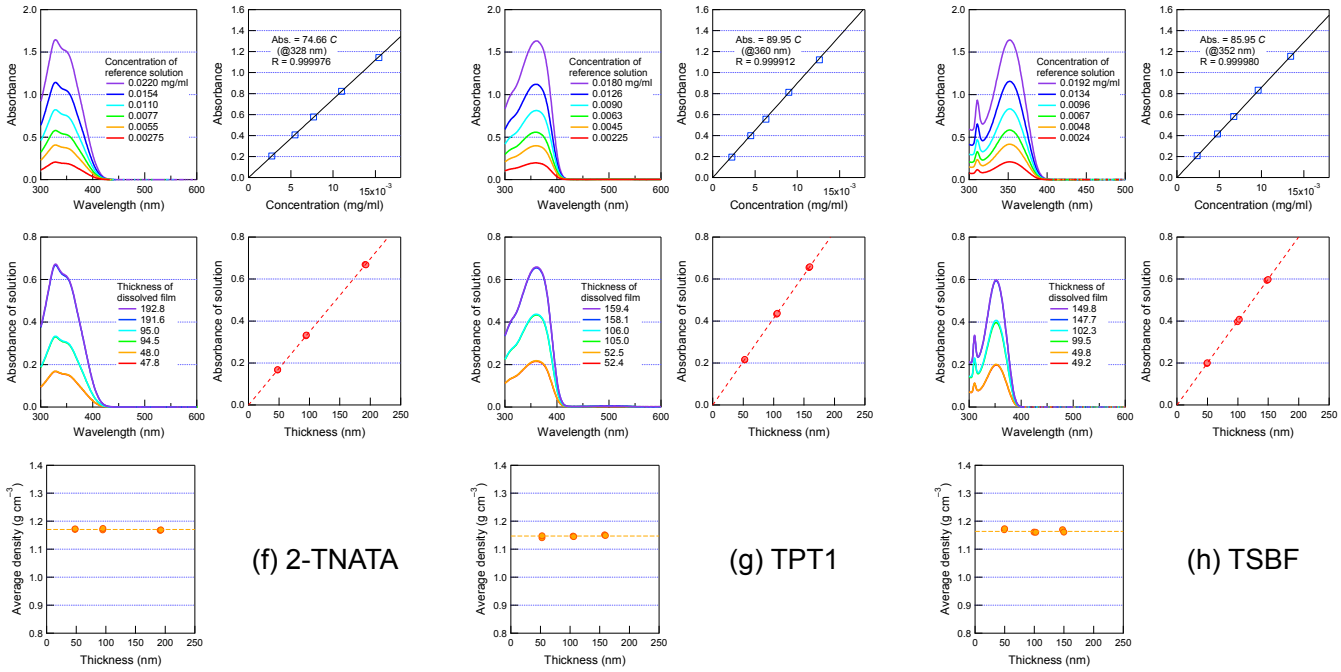

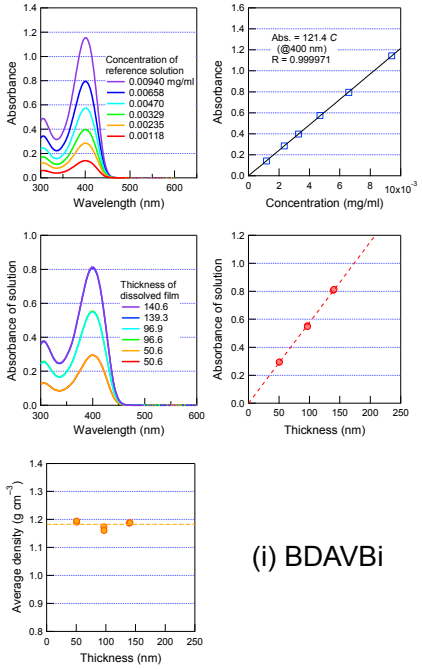

Fig. S1(f)–(i) UV-vis absorption spectra of reference solutions and solutions of dissolved vacuum-deposited films of (f) 2-TNATA, (g) TPT1, (h) TSBF, and (i) BDAVBi. Each material has five figures. For each, the upper left shows the absorption spectra of the reference solutions, and the upper right shows the calibration line. The central left shows the absorption spectra of the solutions of the dissolved films, and the central right shows the dependence of the absorbance on film thickness. The lower left shows the density of films with different thicknesses.

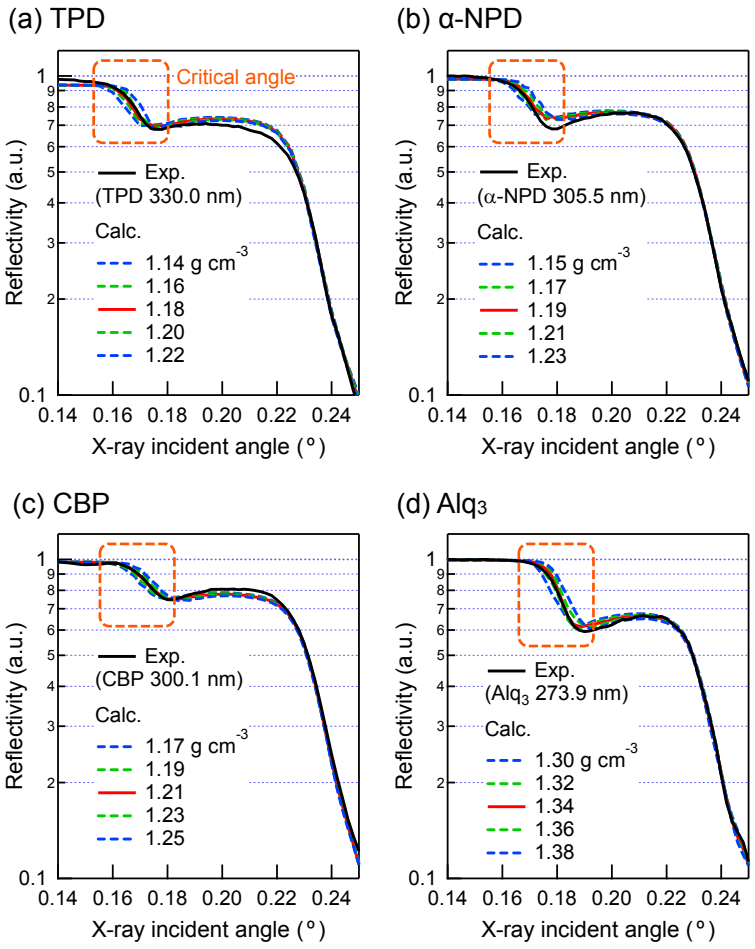

Fig. S2 XRR patterns of vacuum-deposited films of (a) TPD, (b) α-NPD, (c) CBP, and (d) Alq_3 with a thickness of ~300 nm. The theoretical curves for the density within an error of ±0.04 g cm^{-3} are also shown. These results indicate that our estimations with an error of ±0.04 g cm^{-3} are reliable.

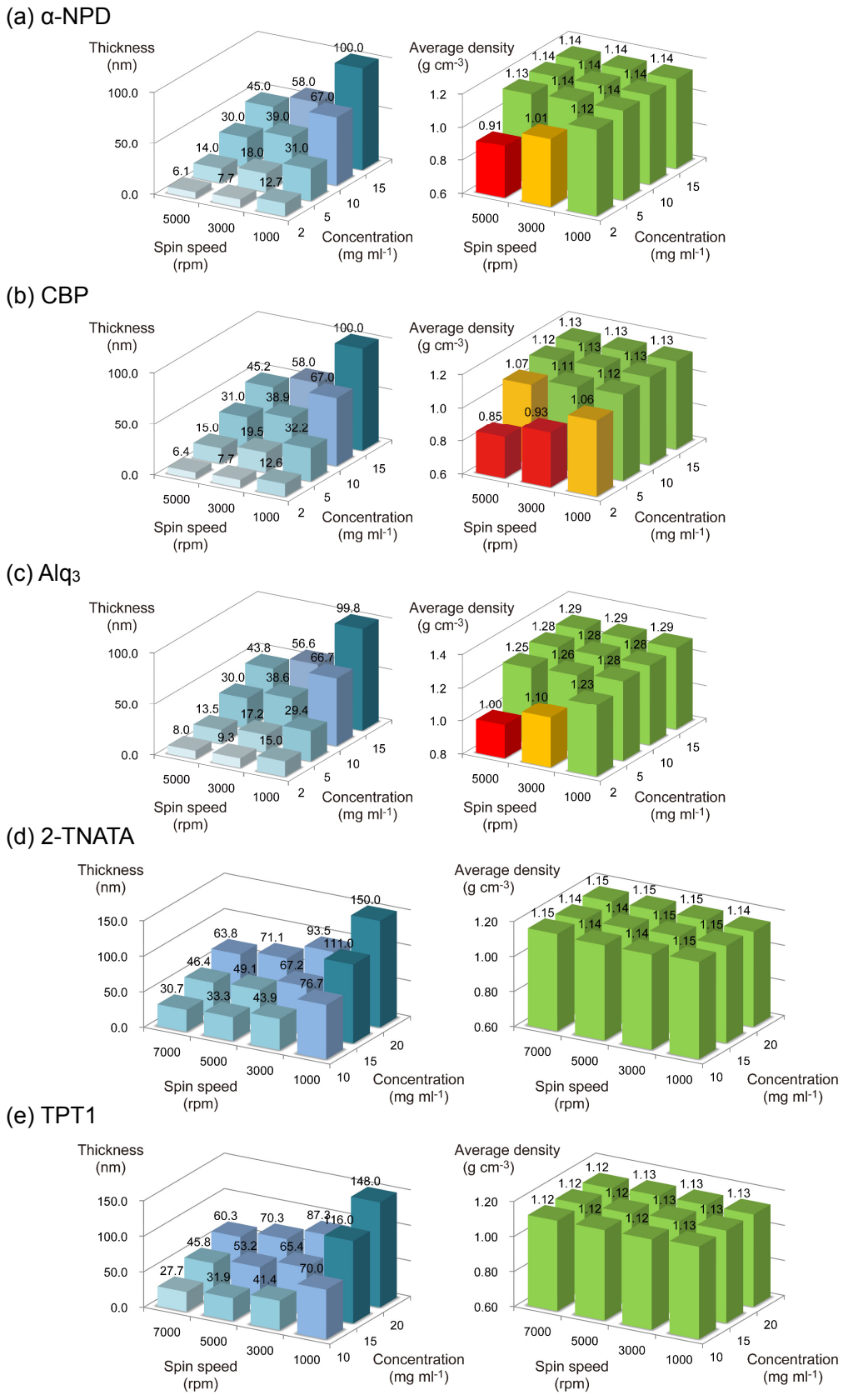

Fig. S3 Thicknesses and film densities of spin-coated films of (a) α-NPD, (b) CBP, (c) Alq_3, (d) 2-TNATA, and (e) TPT1 fabricated using chloroform as the solvent with different spin speeds and solution concentrations.

(a) Toluene

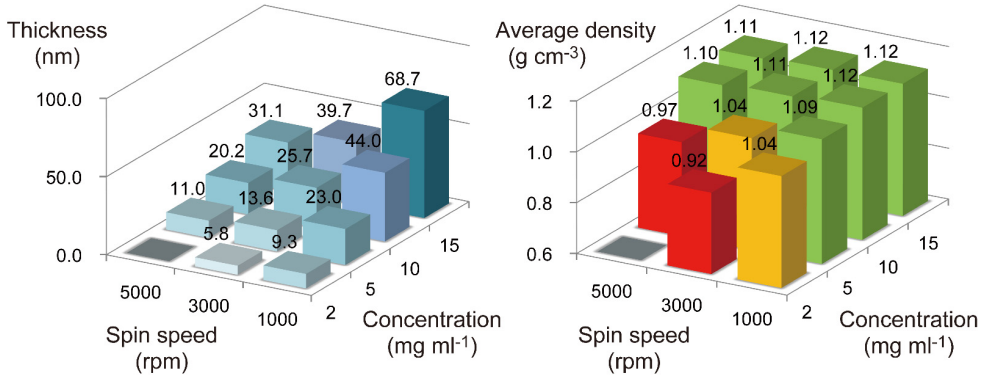

(b) Chlorobenzene

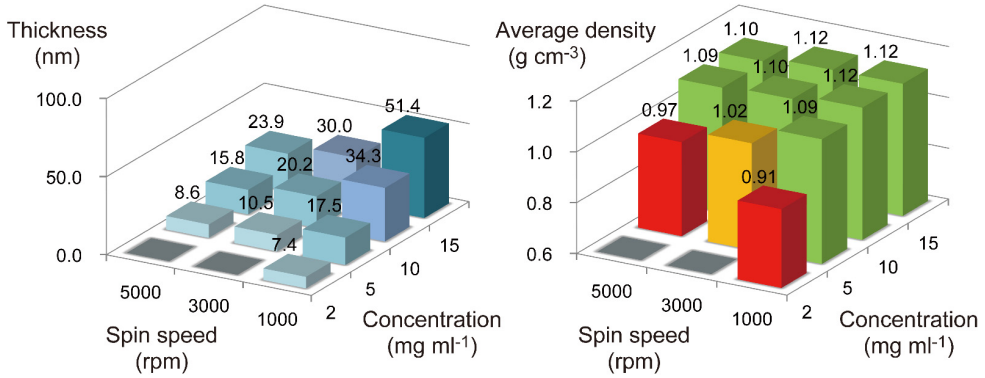

(c) *o*-Dichlorobenzene

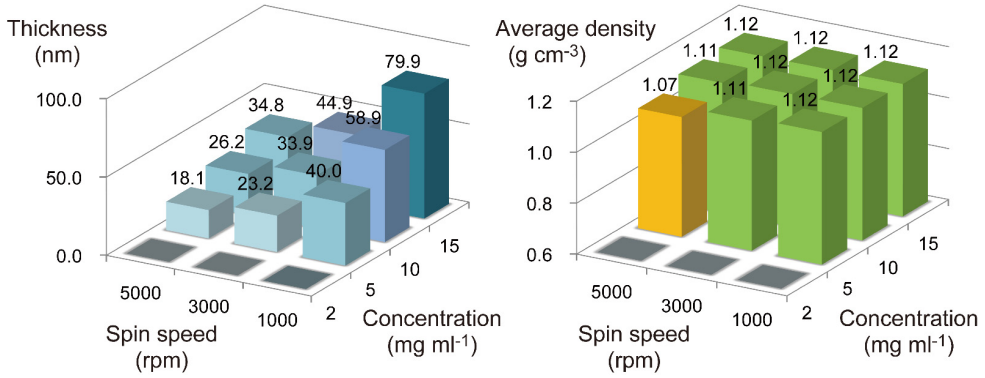

Fig. S4 Thicknesses and film densities of spin-coated TPD films fabricated using (a) toluene, (b) chlorobenzene, and (c) *o*-dichlorobenzene as the solvent with different spin speeds and solution concentrations. These results show that the converged values for density are independent of the type of solvent.

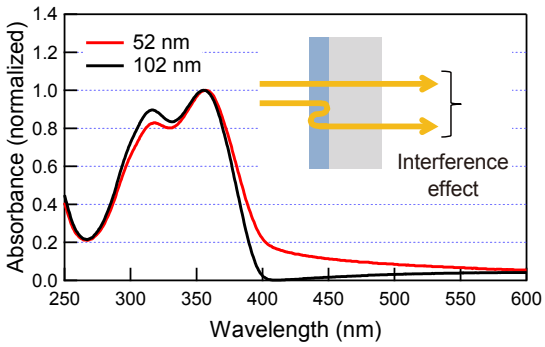

Fig. S5 Normalized absorption spectra of vacuum-deposited TPD films with thicknesses of 52.3 and 102.2 nm. Although the only difference between the two films is the thickness, the spectral shapes obtained by measurements using a spectrophotometer are different because the film thickness influences the interference effect.

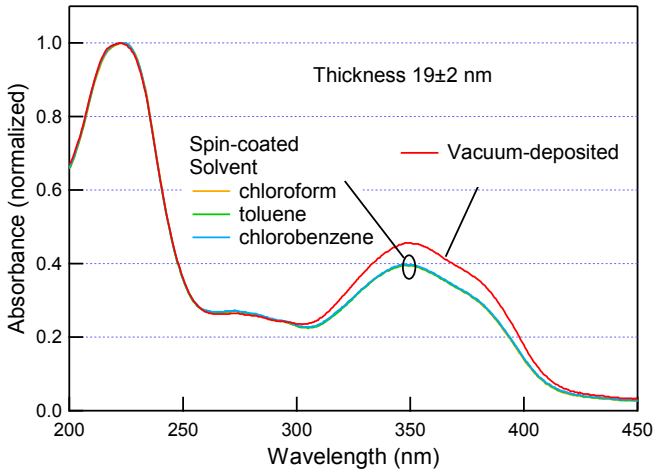

Fig. S6 Normalized absorption spectra of spin-coated α-NPD films fabricated using three different solvents and vacuum-deposited α-NPD films. All films had approximately the same thickness of 19±2 nm: 17.2 nm (chloroform), 18.9 nm (toluene), 19.8 nm (chlorobenzene), and 17.6 nm (vacuum-deposited film).

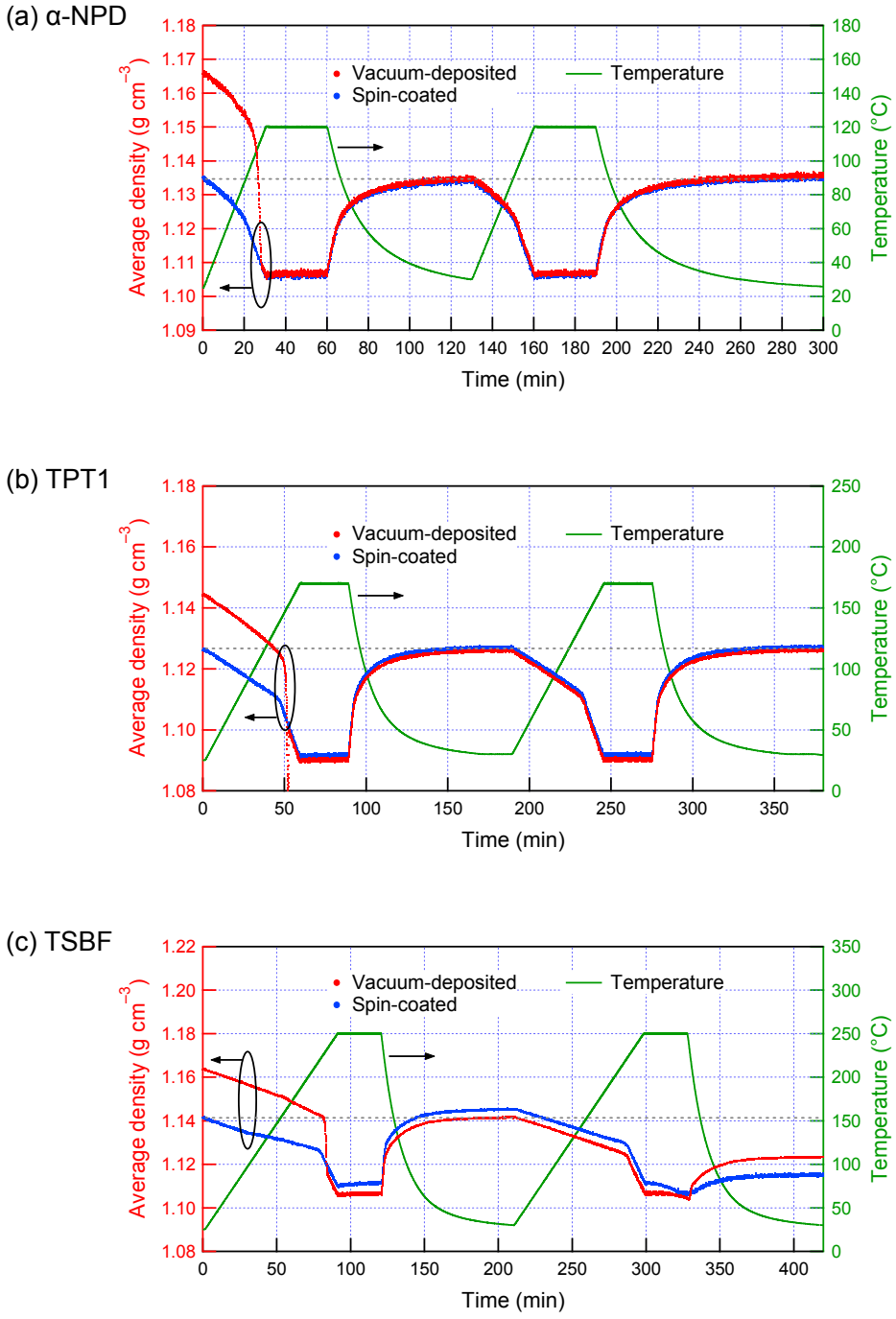

Fig. S7 Changes of the densities of vacuum-deposited (red) and spin-coated (blue) films of (a) α-NPD (with a thickness of ~65 nm), (b) TPT1 (~110 nm), and (c) TSBF (~105 nm) during heating-cooling cycles. The temperature during the cycles is also shown (green). The gray dotted horizontal lines show the identical densities of the transition-experienced vacuum-deposited film and the spin-coated film at room temperature. Although the density at room temperature of the TSBF films seem to decrease after the second cycle, this is caused by crystallization, which increases the roughness of the film surface and lowers apparent density.

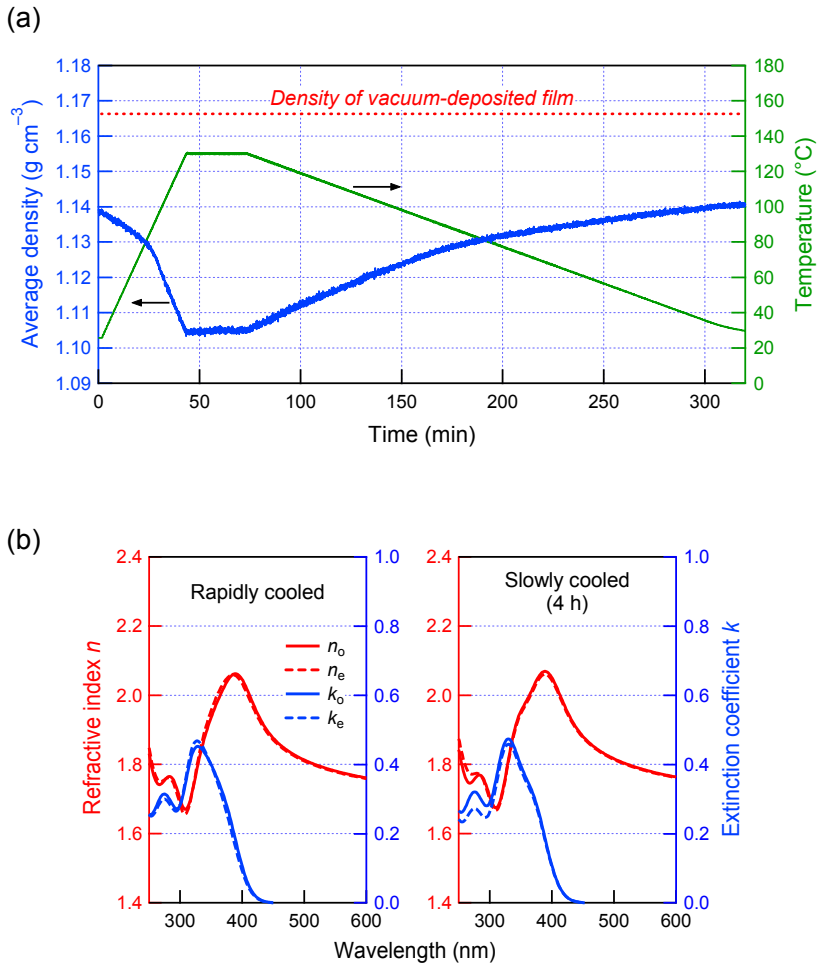

Fig. S8 Effects of slow cooling over 4 h on (a) the density of a spin-coated α-NPD film after transition and (b) the molecular orientation in spin-coated 2-TNATA films after transition. In (a), the change of density of the spin-coated α-NPD films in the slow cooling process is shown. The films were 62.5-nm thick. The green line shows the temperature during the cycles with a very slow cooling process that took 4 h. The red dotted horizontal line shows the density of the vacuum-deposited α-NPD film at room temperature. The results reveal that the slow cooling process cannot compensate the difference between the densities of the vacuum-deposited and spin-coated films. In (b), the anisotropic optical constants of transition-experienced 2-TNATA films that have been cooled rapidly and slowly are shown. Two spin-coated 2-TNATA films with original thicknesses of 103.0 and 111.0 nm were annealed at 130 °C for 30 min, and then one was rapidly cooled on a metal plate at room temperature, while the other was slowly cooled over 4 h using a temperature-control stage. The red solid and broken lines show the refractive indices in the horizontal and vertical directions (n_o and n_e), respectively, and the blue solid and broken lines show the extinction coefficients in the horizontal and vertical directions (k_o and k_e), respectively. The result of no significant difference indicates that the slow cooling process cannot change the random molecular orientation in the spin-coated film.

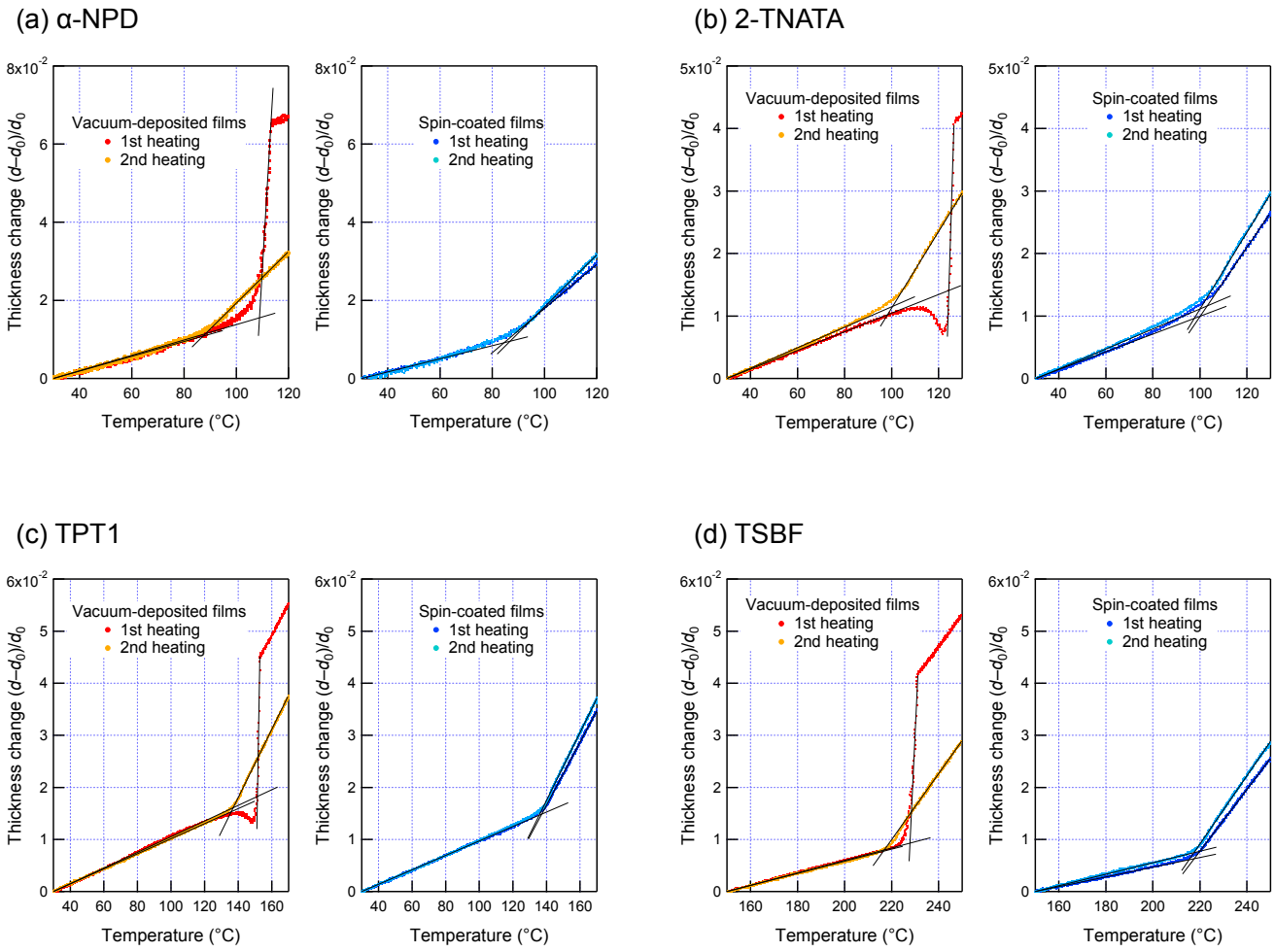

Fig. S9 Thickness changes of vacuum-deposited and spin-coated films of (a) α-NPD, (b) 2-TNATA, (c) TPT1, and (d) TSBF during the first and second heating processes. The slopes are the thermal expansion coefficients, and the cross points of the slope lines (black lines) show the transition temperatures.

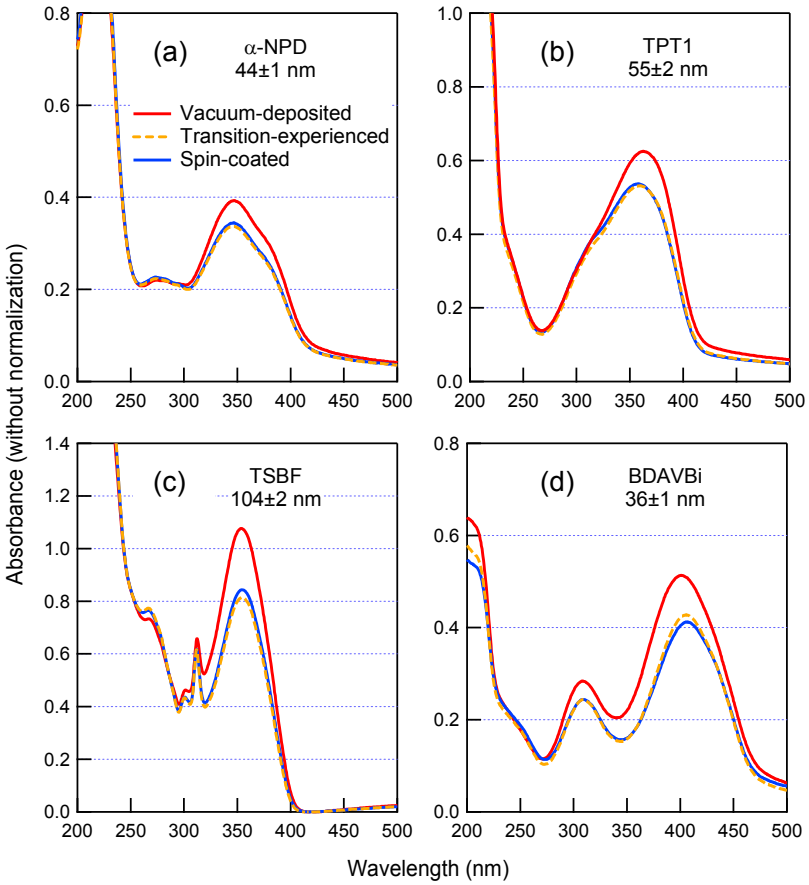

Fig. S10 Absorption spectra without normalization of as-prepared vacuum-deposited films, transition-experienced vacuum-deposited films, and spin-coated films of (a) α-NPD, (b) TPT1, (c) TSBF, and (d) BDAVBi. The original thicknesses of the vacuum-deposited and spin-coated films were approximately the same (see Table S1 for details). The results show that the absorbance of the vacuum-deposited films decreases after the transition because of the randomization of molecular orientation, and also that the absorption spectra of the transition-experienced and spin-coated films are identical.

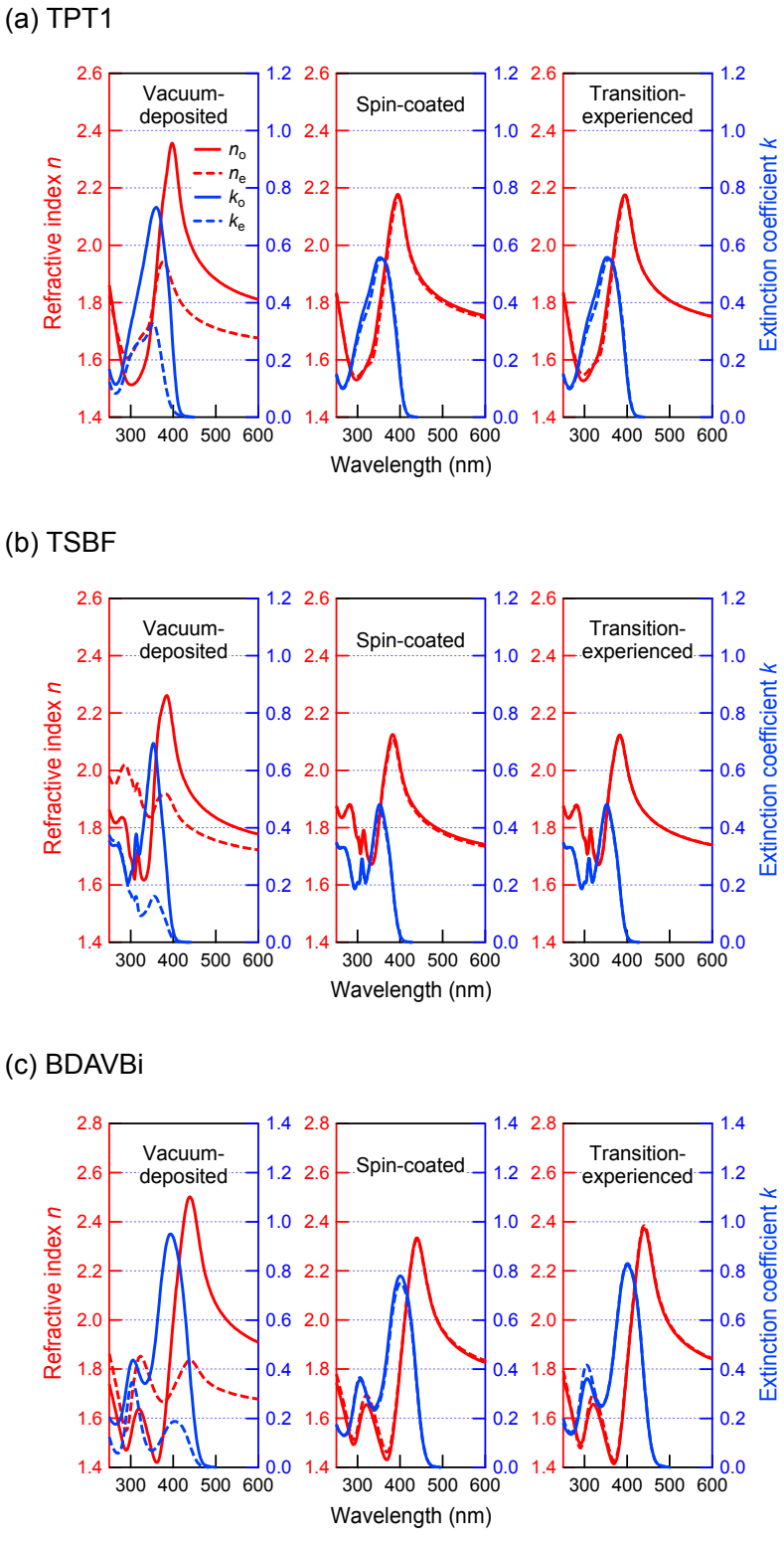

Fig. S11 Anisotropic optical constants of as-prepared vacuum-deposited films, spin-coated films, and transition-experienced vacuum-deposited films of (a) TPT1, (b) TSBF, and (c) BDAVBi. The thicknesses of the films were 96–116 nm (see Table S1 for details). The red solid and broken lines show the refractive indices in the horizontal and vertical direction (n_o and n_e), respectively, and the blue solid and broken lines show the extinction coefficients in the horizontal and vertical direction (k_o and k_e), respectively. The results reveal a high degree of horizontal orientation in the vacuum-deposited films and the similarity of the spin-coated and transition-experienced films with random orientation.

(a) TPT1/chloroform

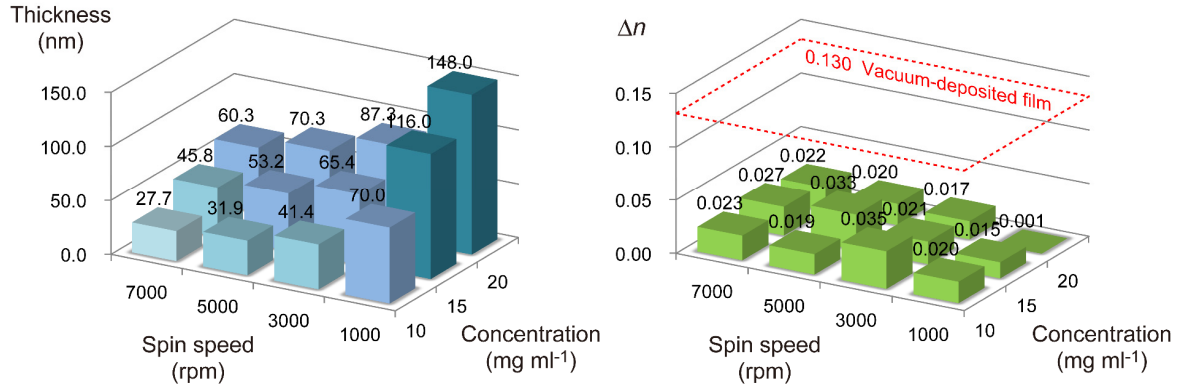

(b) TPT1/toluene

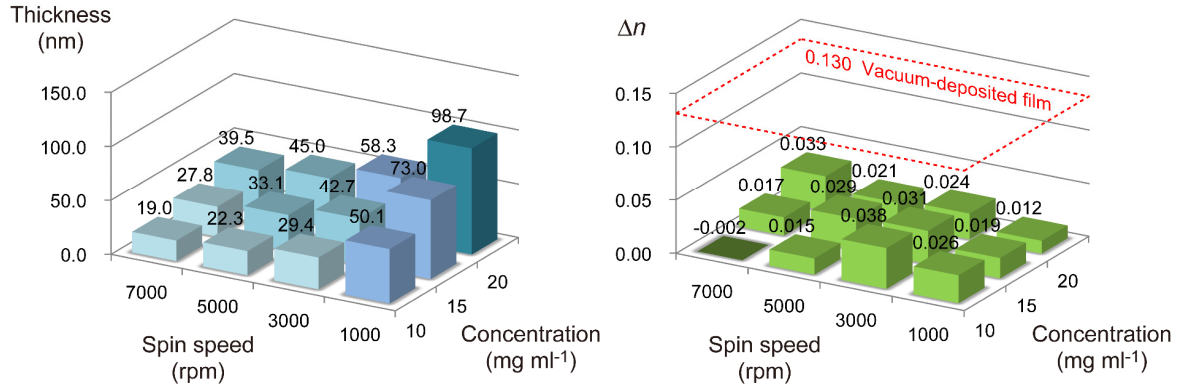

Fig. S12 Thicknesses and birefringences of spin-coated TPT1 films fabricated using (a) chloroform and (b) toluene as the solvent under with different spin speeds and solution concentrations. The birefringence of the vacuum-deposited TPT1 film is also shown (red dotted line). The results show that the molecular orientation in the spin-coated films is nearly random over the wide range of spin-coating conditions investigated, and the degree of horizontal molecular orientation in the spin-coated films is much lower than that in the vacuum-deposited films.

(a) TPT1/chloroform

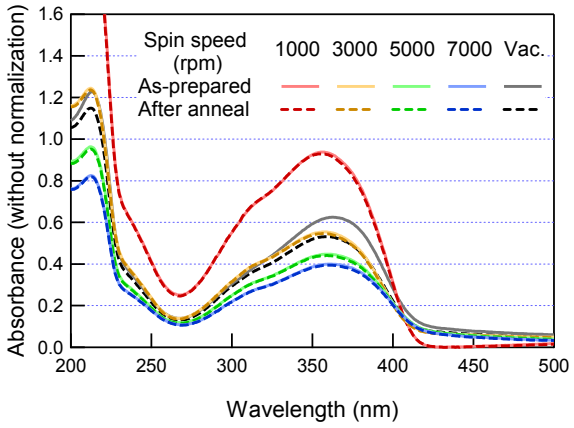

(b) TPT1/toluene

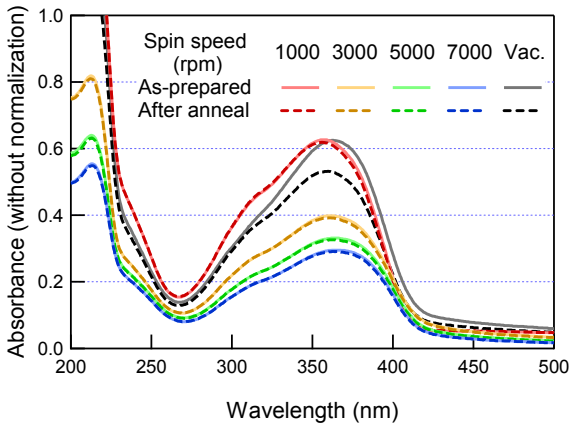

Fig. S13 Absorption spectra without normalization of as-prepared and transition-experienced spin-coated TPT1 films fabricated using (a) chloroform and (b) toluene as the solvent with a solution concentration of 15 mg ml^{-1} and different spin speeds. Absorption spectra of as-prepared and transition-experienced vacuum-deposited TPT1 films with a thickness of ~50 nm are also shown.

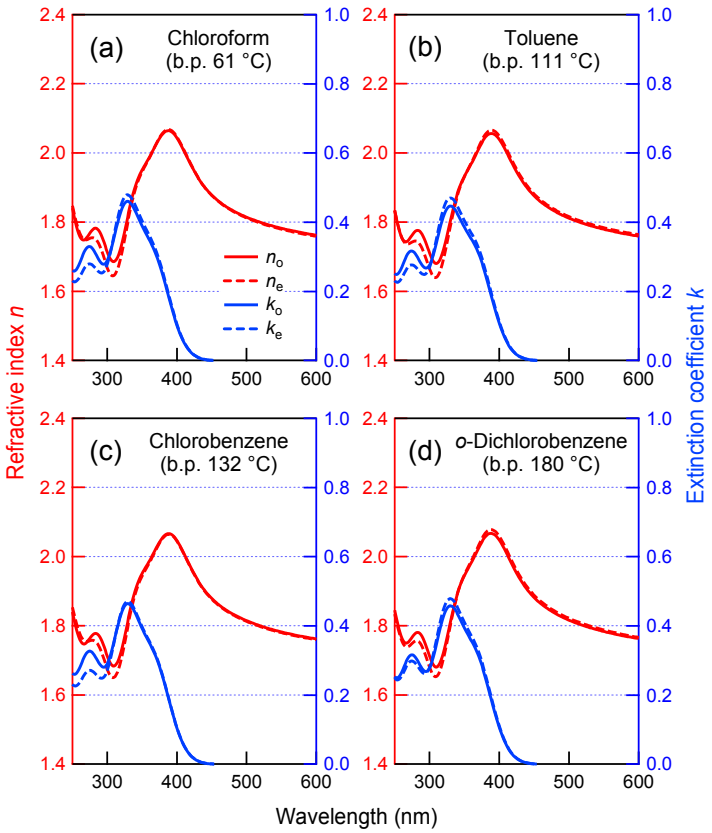

Fig. S14 Anisotropic optical constants of spin-coated 2-TNATA films fabricated using (a) chloroform, (b) toluene, (c) chlorobenzene, and (d) *o*-dichlorobenzene as the solvent. The thicknesses of the films were 100–110 nm (see Table S1 for details). The red solid and broken lines show the refractive indices in the horizontal and vertical directions (n_o and n_e), respectively, and the blue solid and broken lines show the extinction coefficients in the horizontal and vertical directions (k_o and k_e), respectively. The results reveal that there is no significant dependence of optical constants on the type of solvent.

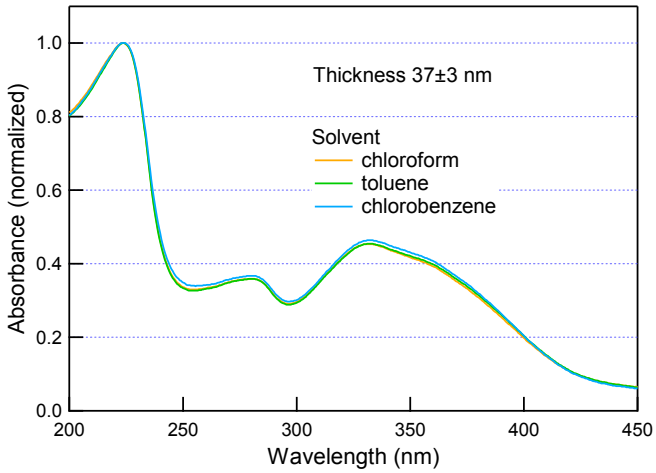

Fig. S15 Normalized absorption spectra of spin-coated 2-TNATA films fabricated using three different solvents. All films had approximately the same thickness of 37±3 nm: 35.1 nm (chloroform), 39.7 nm (toluene), and 35.4 nm (chlorobenzene). The results show that there was no significant dependence of the absorption spectra on the type of solvent.

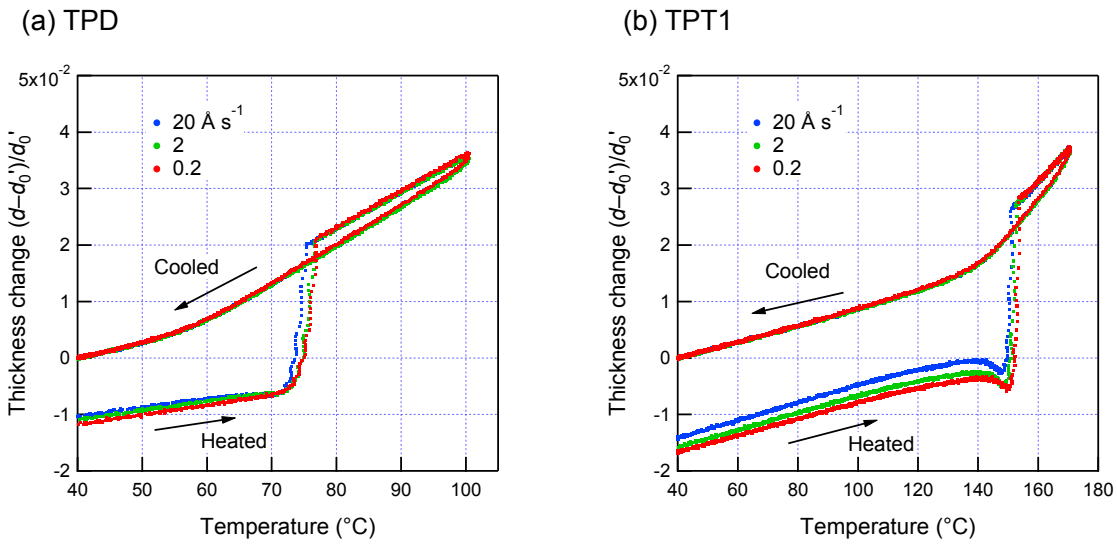

Fig. S16 Thickness changes of vacuum-deposited (a) TPD and (b) TPT1 films fabricated at different deposition rates of 0.2, 2, and 20 Å/s during a heating and cooling cycle. To compare the densities of the as-prepared films, the thicknesses at 40 °C after cooling d_0' are used as the standards for normalization.

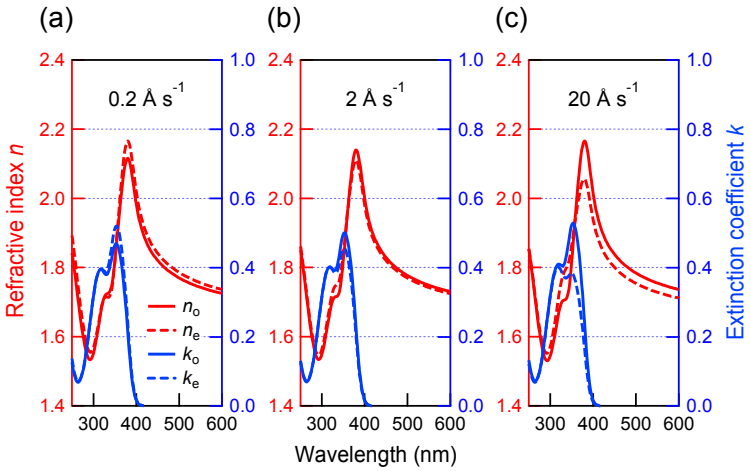

Fig. S17 Anisotropic optical constants of vacuum-deposited TPD films with a thickness of ~100 nm fabricated at deposition rates of (a) 0.2, (b) 2, and (c) 20 Å/s. The red solid and broken lines show the refractive indices in the horizontal and vertical directions (n_o and n_e), respectively, and the blue solid and broken lines show the extinction coefficients in the horizontal and vertical directions (k_o and k_e), respectively.

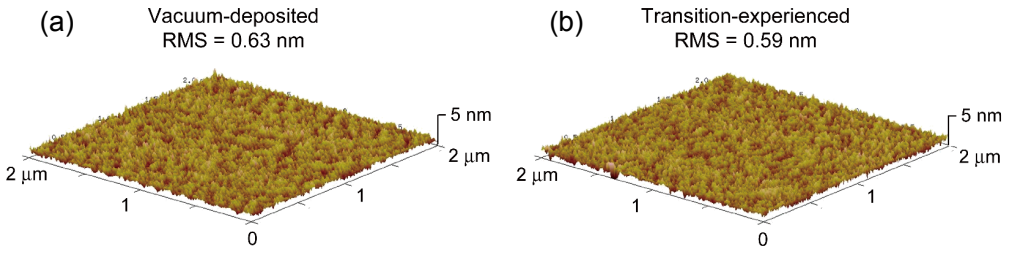

Fig. S18 Atomic force microscope images of the surface of a vacuum-deposited TPD film (a) before and (b) after annealing at 100 °C for 30 min. The sample film with a thickness of 49.0 nm was deposited on a Si substrate. These images show that the surface roughness of vacuum-deposited TPD films does not become large even after the transition induced by heating.

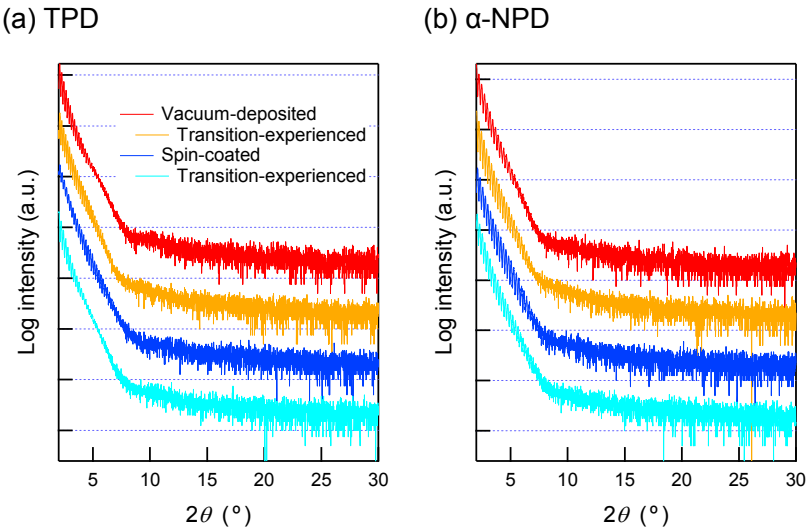

Fig. S19 Out-of-plane X-ray diffraction (XRD) patterns of vacuum-deposited and spin-coated TPD and α-NPD films on a Si substrate. The XRD patterns of the films after transition were also measured. The thickness of the TPD films was ~46 nm, and that of the α-NPD films was ~37 nm. There is no apparent diffraction peak in the patterns, showing that all of these films remain amorphous without crystallization even after the transition induced by heating.